



TITLE:

# A Study of Super-High Speed Machining

AUTHOR(S):

OKUSHIMA, Keiji; HITOMI, Katsundo; ITO, Shuntaro

---

CITATION:

OKUSHIMA, Keiji ...[et al]. A Study of Super-High Speed Machining. Memoirs of the Faculty of Engineering, Kyoto University 1964, 26(2): 85-109

ISSUE DATE:

1964-06-10

URL:

<http://hdl.handle.net/2433/280591>

RIGHT:

# A Study of Super-High Speed Machining

By

Keiji OKUSHIMA\*, Katsundo HITOMI\*, and Shuntaro ITO\*\*

(Received January 31, 1964)

This paper is concerned with the fundamental study of super-high speed machining. Cutting tests were performed on carbon steel with carbide, ceramic, and cermet tools to investigate the fundamental problems such as tool forces, tool life, surface roughness, etc. at super-high speeds (above the conventional cutting speed) obtained easily by the latest high-speed precision lathe, and to find out the possibility of practical use of super-high speed machining in machine shops. It was found that a certain grade of the ceramic tool has a great possibility of being used for super-high speed machining. Super-high speed machining operation produced an excellent surface finish, increasing the productivity of finish operation, but the tool life at super-high speeds was short at the present stage. The development of tool materials with high heat resistance and machine tools with high rigidity enough for super-high speeds is expected. Cutting fluids supplied to super-high speed machining increased surface finish slightly, but decreased tool life.

## 1. Introduction

With the progress of machine tools and cutting tools, the cutting speed in machining operation has recently increased and the usual cutting speed in the practical shop work has reached about 300 m/min. In order to increase productivity, high speed machining operation above this conventional speed range has been investigated. This is what is called ultra-high speed machining.<sup>1)2)3)</sup> For example, the ultra-high speed cutting tests were performed at cutting speeds of 15000 to 360000 fpm, using an explosively actuated apparatus.<sup>4)</sup>

The most important advantages of the super-high speed machining are to improve the productivity of the machining operation and to produce an excellent surface finish and dimensional accuracy. In addition, it is expected by this machining operation to machine those alloys which missiles and high-performance aircrafts require to withstand high temperatures. On the other hand, the super-high speed machining has disadvantages: rapid wear of cutting tools and vibration of machine tools.

---

\* Department of Precision Mechanics

\*\* Sumitomo Metal Company

The purposes of this study of super-high speed machining here reported were to investigate the machining operations at super-high speeds (above the conventional cutting speed) which were easily obtained by the latest high-speed lathe, and to find out the possibility of its practical use. Super-high speed cutting tests were conducted on carbon steels with carbide, cermet, and ceramic cutting tools, and the fundamental problems on high speed machining operations were investigated regarding tool forces, tool wear, tool life, surface roughness, effect of cutting fluids, etc.

## 2. Experimental Procedure

All the tests were conducted in a VDF high speed lathe (Heidenreich and Harbeck; swing 520 mm, center distance 1000 mm, power 15 kW) equipped with a Ward-Leonard variable speed drive. This produces high cutting speed range required for the purpose of this investigation.

Tool materials used were tungsten carbide, cermet, and ceramic. A clamp-type tool holder and square throw-away inserts were employed. Tool geometry and insert dimensions were:

Back rake angle	:	-5 deg
Side rake angle	:	-5 deg
End relief angle	:	5 deg
Side relief angle	:	5 deg
End cutting edge angle	:	15 deg
Side cutting edge angle	:	15 deg
Nose radius	:	0.8 mm
Insert dimensions (square)	:	12.7 × 3.2 mm for carbide 12.7 × 4.8 mm for cermet and ceramic

Precision-ground inserts were used as obtained from the manufacturer, and each run was started with a new cutting edge.

Work materials tested were cylindrical billets of carbon steel S45C. The chemical composition and the hardness of the test material are shown in Table 1.

During the tests three components of tool forces, i.e., principal cutting force, radial cutting force, and feed cutting force were measured with a three-component

Table 1. Chemical composition and hardness of work material tested (S45C).

Chemical composition (%)							Brinell Hardness
C	Mn	Si	Cu	Cr	S	P	
0.48	0.76	0.32	0.14	0.11	0.020	0.015	274

strain-gage-type tool dynamometer<sup>5)</sup> and recorded on oscillograph paper. The wear process of tool materials was observed with a Nikon Toolmakers' microscope (Nippon Kogaku Optical Co.), interrupting cutting operation at a certain period. After the tests the roughness of the machined surfaces was measured with a Talysurf surface roughness indicator (Taylor-Hobson Co.). Tests were generally run under the following conditions (detail cutting conditions are indicated in each subject):

Depth of cut : 0.10 to 0.90 mm  
 Feed : 0.012 to 0.100 mm/rev  
 Cutting speed : 150 to 3000 m/min

### 3. Tool Force Measurement

Cutting tests were run dry on carbon steel, S45C, about 50 mm long, with several kinds of tool materials (Table 2) to investigate tool force pattern in relation to cutting speed at super-high speeds. Feed rate and depth of cut were kept constant: 0.05 mm/rev and 0.50 mm, respectively. Cutting speed was varied from 200 m/min to 2000 m/min.

Table 2. Tool materials used.

Nomenclature	Tool material	Manufacturer
C-1	Tungsten carbide (steel cutting grade)	Company A
C-1*†	Tungsten carbide (steel cutting grade)	Company A
C-2	Tungsten carbide (steel cutting grade)	Company A
C-3	Tungsten carbide (cast iron cutting grade)	Company A
T-1	Cermet (titanium carbide)	Company A
O-1	Ceramic (aluminum oxide)	Company A
O-2	Ceramic (aluminum oxide)	Company B

† This is the same material as C-1 except a positive side rake angle of 5 deg.

Fig. 1 shows tool force pattern in relation to cutting speed for the steel cutting grade carbide C-1. Three force components at the beginning of each cut were almost constant or rather decreased with an increase in cutting speed. Tool forces increased as the cutting time elapsed, and those at the final stage of about 50 mm cut increased with an increase in cutting speed. This tendency is remarkable for radial and feed force components at cutting speeds above 1000 m/min. An example for force variation with cutting time for carbide C-1 is shown in Fig. 2. Regarding the cast iron cutting grade carbide C-3, as shown in Fig. 3, the large force increase at the final stage was observed at a cutting speed much lower than in the case of the steel cutting grade carbide C-1.

Tool force pattern for the cermet tool T-1 are shown in Fig. 4. The initial

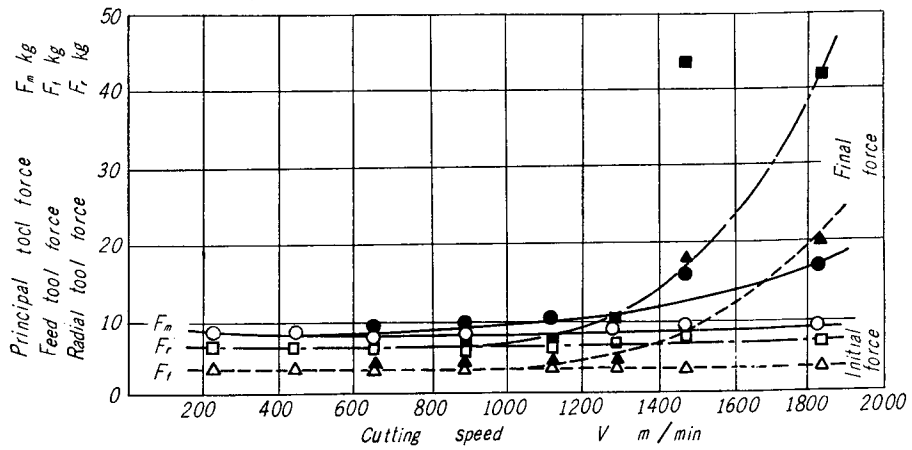


Fig. 1. Relationship between cutting speed and tool forces [Tool material, carbide C-1 (steel cutting grade); tool geometry,  $-5^\circ$ ,  $-5^\circ$ ,  $5^\circ$ ,  $5^\circ$ ,  $15^\circ$ ,  $15^\circ$ , 0.8 mm; work material, S45C; depth of cut, 0.50 mm; feed, 0.05 mm/rev; dry]

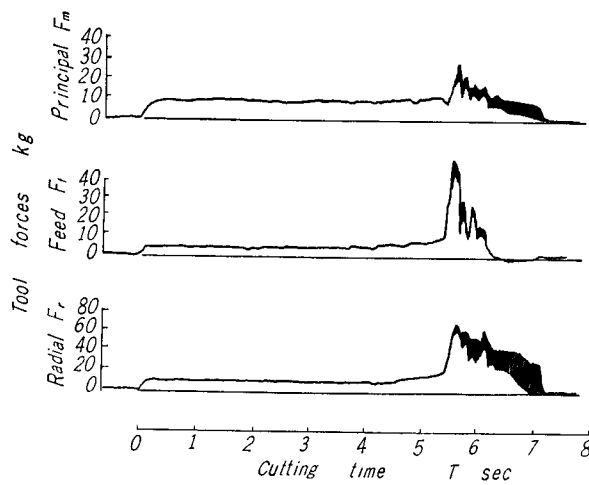


Fig. 2. An example of tool force variation with cutting time [Tool material, carbide C-1 (steel cutting grade); tool geometry,  $-5^\circ$ ,  $-5^\circ$ ,  $5^\circ$ ,  $5^\circ$ ,  $15^\circ$ ,  $15^\circ$ , 0.8 mm; work material, S45C; depth of cut, 0.50 mm; feed, 0.05 mm/rev; cutting speed, 1475 m/min; dry]

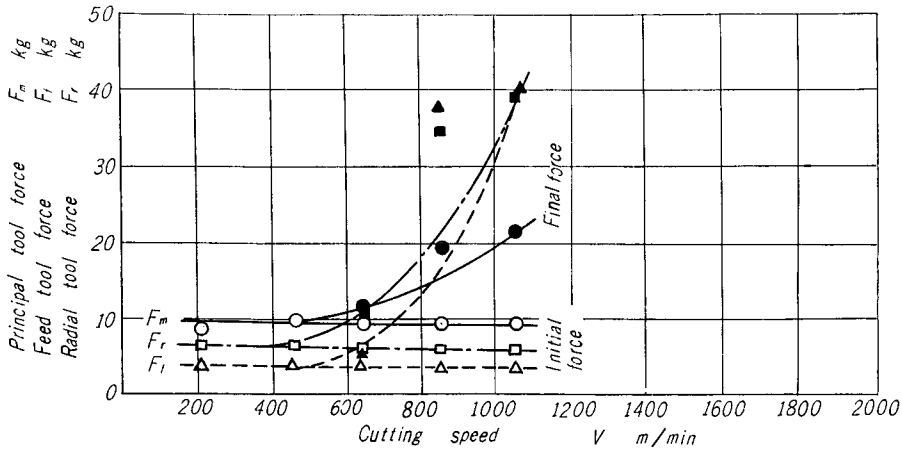


Fig. 3. Relationship between cutting speed and tool forces [Tool material, carbide C-3 (cast iron cutting grade); tool geometry,  $-5^\circ$ ,  $-5^\circ$ ,  $5^\circ$ ,  $5^\circ$ ,  $15^\circ$ ,  $15^\circ$ , 0.8 mm; work material, S45C; depth of cut, 0.50 mm; feed, 0.05 mm/rev; dry]

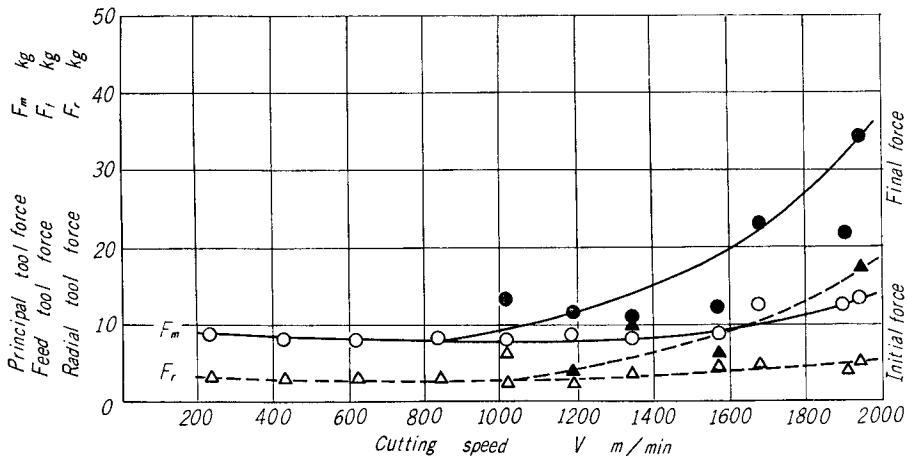


Fig. 4. Relationship between cutting speed and tool forces [Tool material, cermet T-1; tool geometry,  $-5^\circ$ ,  $-5^\circ$ ,  $5^\circ$ ,  $5^\circ$ ,  $15^\circ$ ,  $15^\circ$ , 0.8 mm; work material, S45C; depth of cut, 0.50 mm; feed, 0.05 mm/rev; dry]

tool forces decreased slightly with an increase in cutting speed. The force increase from the beginning of cut until the final stage was a little smaller than for the steel cutting grade carbide C-1. Tool force variation with cutting time for the cermet T-1 is shown in Fig. 5.

Compared with the carbide and the cermet tools mentioned above, the ceramic tool O-1 showed a different tendency in tool force pattern in relation to cutting speed (Fig. 6). Tool forces were almost constant with an increase in cutting

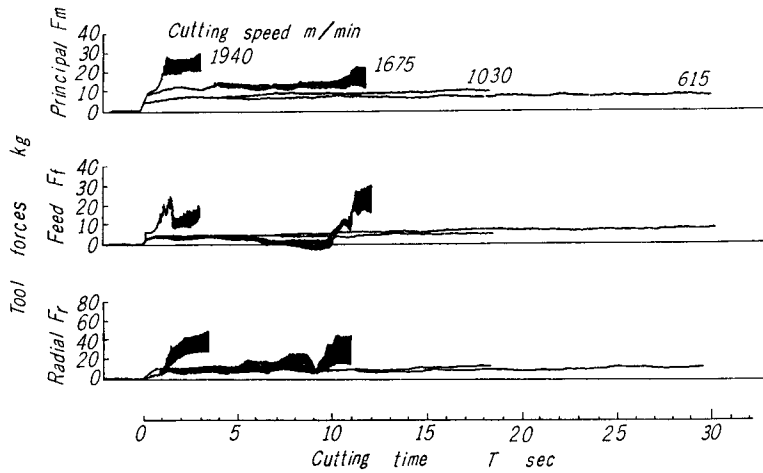


Fig. 5. An example of tool force variation with cutting time [Tool material, cermet T-1; tool geometry,  $-5^\circ, -5^\circ, 5^\circ, 5^\circ, 15^\circ, 15^\circ, 0.8$  mm; work material, S45C; depth of cut, 0.50 mm; feed, 0.05 mm/rev; dry]

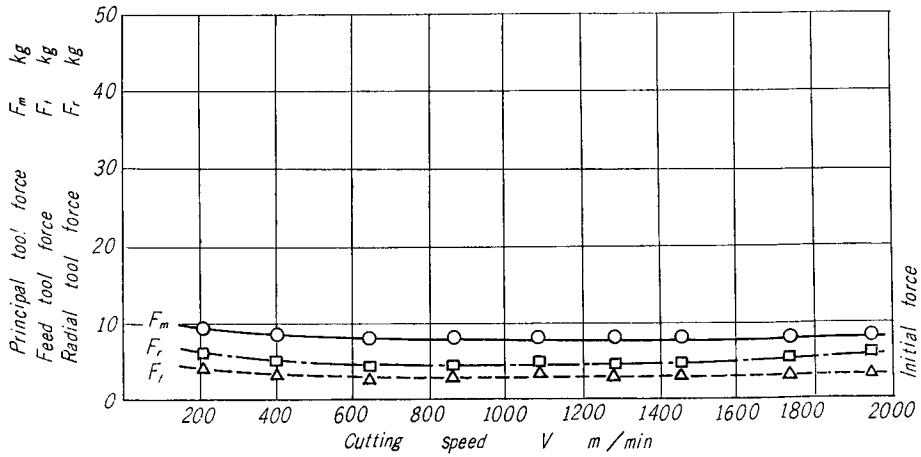


Fig. 6. Relationship between cutting speed and tool forces [Tool material, ceramic O-1; tool geometry,  $-5^\circ, -5^\circ, 5^\circ, 5^\circ, 15^\circ, 15^\circ, 0.8$  mm; work material, S45C; depth of cut, 0.50 mm; feed, 0.05 mm/rev; dry]

speed and no force increase with cutting time was recognized throughout the cutting speeds tested in this short-period cutting operation. This indicates that this kind of ceramic tool is superior in performance of super-high speed cutting to the carbide and the cermet tools. Thus, great possibility for super-high speed machining is expected with the ceramics.

The above experiments indicate that the initial tool forces are almost the same with various tool materials tested. However, the final tool forces at high

speeds differ so much for different tool materials. Therefore, the amount of force increases with cutting time is one of the criterions to determine an adequate tool material for super-high speed machining. Fig. 7 shows the cutting time up to the beginning of force increases in relation to cutting speeds for various cutting tool materials. This is one of the tool-life curves. The cutting time up to the beginning of force increase decreases with an increase in cutting speed.

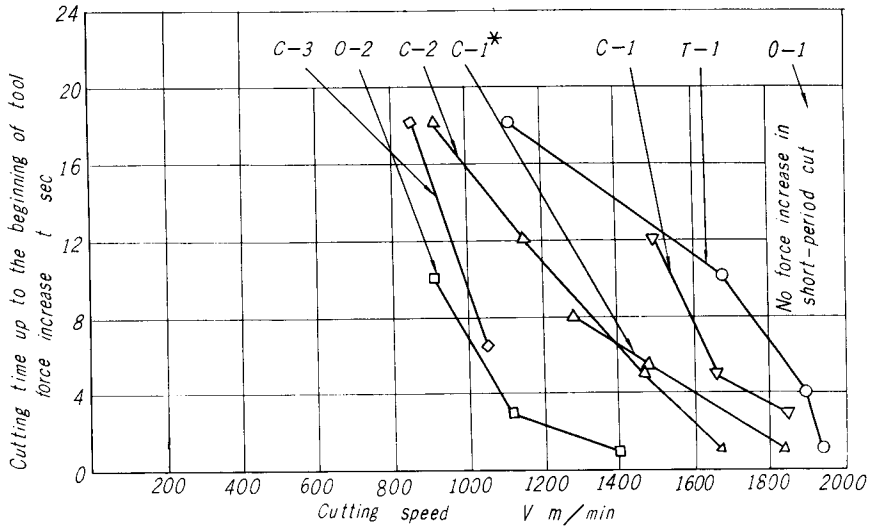


Fig. 7. Relationship between cutting speed and cutting time up to the beginning of tool force increase [Work material, S45C; depth of cut, 0.50 mm; feed, 0.05 mm/rev; dry]

The tool material having the curve located at the increasing side of cutting speed in this figure has high performance of super-high speed machining. It appears from this figure that the ceramic tool O-1 is most suitable to super-high speed machining and the cermet tool T-1 ranks next to it. There is almost no possibility of super-high speed machining with carbide tools. The use of carbide tools is limited to cutting speeds up to several hundred meters per minute.

#### 4. Tool Wear and Tool Life Tests

Tool life is an important factor determining the possibility of super-high speed machining in practical manufacturing processes.

Tool-life tests were performed at super-high speeds on carbon steel S45C with carbide C-1, cermet T-1, and ceramic O-1, and the wear processes were investigated. Depth of cut and feed rate were kept constant : 0.50 mm and 0.05 mm/rev, respectively. Cutting speed was varied ; 300 to 1500 m/min for carbide C-1, 200



to 2500 m/min for cermet T-1, and 300 to 3000 m/min for ceramic O-1. The tool-life criterion in this experiment was a maximum flank wear land of 0.40 mm.

An example of the tool wear process at super-high speeds are shown in Fig. 8. The comma-shaped crater wear which expanded to the side cutting edge was clearly observed on the tool face for the carbide cutting tool C-1. This crater wear occurred from the very beginning of cut and grew rapidly with cutting time. The higher the cutting speed, the greater the rate of increase in the crater wear.

On the other hand, the crater wear did not clearly occur with the ceramic tool O-1 even at super-high speeds. This is because the aluminum oxide which

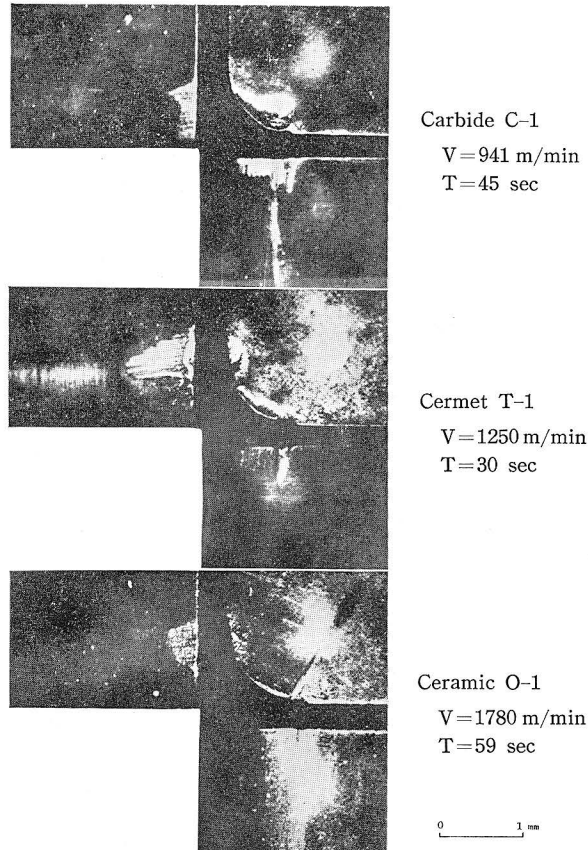


Fig. 8. Examples of tool wear process in super-high speed machining [Tool material, carbide C-1 (steel cutting grade), cermet T-1, and ceramic O-1; tool geometry,  $-5^\circ$ ,  $-5^\circ$ ,  $5^\circ$ ,  $5^\circ$ ,  $15^\circ$ ,  $15^\circ$ , 0.8 mm; work material, S45C; depth of cut, 0.50 mm; feed 0.05 mm/rev; dry]

is a major ingredient in the ceramic is very stable even at high temperature and high pressure, and the chip flows out without occurrence of adhesion to the tool face. But, since the ceramic tool is rather brittle, the tool face was scratched significantly by the hardened chip and the stripe was clearly observed on the tool face in the direction of chip flow.

The wear process on the tool face for the cermet T-1 was one between those for the carbide C-1 and the ceramic O-1. The arch-shaped crater wear was observed along the cutting edge. The rate of increase in the amount of crater wear was very small for both cermet and ceramic tools. The land of the crater wear was very narrow at super-high speeds for all cutting tool materials. This was mainly because the contact area of the chip on the tool face was located close to the cutting edge.

Examples of the wear process of flank wear for three tool materials are shown in Figs. 9 to 12. It is found from Fig. 9 that the boundary flank wear increased at the greatest rate for the carbide tool C-1. This determined the tool life based upon a flank wear land of 0.40 mm throughout the speed range tested. The higher the cutting speed, the larger the rate of increase in this boundary flank wear.

In the case of the ceramic tool O-1, the chipping wear on the nose of the tool was extremely small (Fig. 10). Its growth remained less than 0.1 mm throughout the super-high speed range tested. This may be a reason why the tool forces did not increase even at the end of tool life and the sharpness of the cutting edge was maintained for longer time for the ceramic O-1 than for other tool materials. At cutting speeds above 2000 m/min, the wear on the front of a tool increased at the greatest rate and determined the tool life [Fig. 10(a)]. But the lower the cutting speed, the larger the rate of increase in the boundary flank wear on the side of a tool [Fig. 10(b)].

Regarding the flank wear for the cermet tool T-1, the chipping wear on the front and the nose was noticeable at super-high speeds, especially above 1250 m/min. This means a sudden decrease in hardness of the tool material at an elevated temperature due to an increase in cutting speed. At cutting speeds below 1000 m/min, the boundary flank wear on the side of a tool was the largest as in the case of the ceramic tool O-1, as shown in Fig. 11.

The flank adhesion was not observed with the carbide tool C-1, while it occurred at the boundary region on the side of both cermet T-1 and ceramic O-1 at low speeds.

Figs. 12 to 14 show typical wear progresses with cutting time for several cutting speeds. It is found from these figures that the primary type of flank

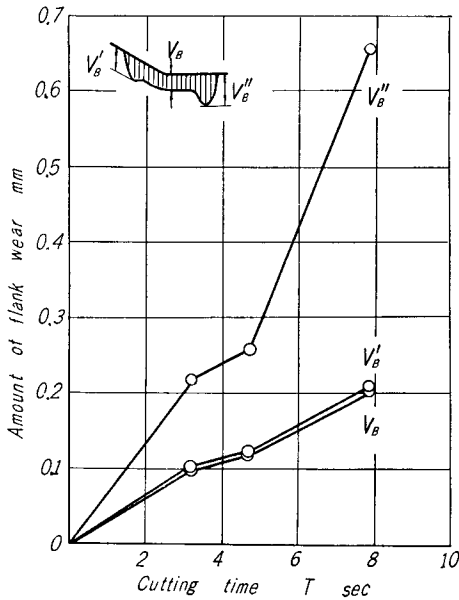


Fig. 9. Progress of flank wear with cutting time for carbide C-1 (steel cutting grade) [Work material, S45C; tool geometry,  $-5^\circ$ ,  $-5^\circ$ ,  $5^\circ$ ,  $5^\circ$ ,  $15^\circ$ ,  $15^\circ$ , 0.8 mm; cutting speed, 1250 m/min; depth of cut, 0.50 mm; feed, 0.05 mm/rev; dry]

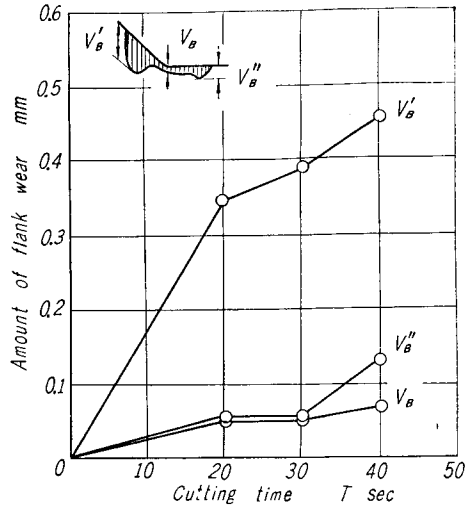


Fig. 10(a). Progress of flank wear with cutting time for ceramic O-1 [Work material, S45C; tool geometry,  $-5^\circ$ ,  $-5^\circ$ ,  $5^\circ$ ,  $5^\circ$ ,  $15^\circ$ ,  $15^\circ$ , 0.8 mm; cutting speed, 2000 m/min; depth of cut, 0.50 mm; feed, 0.05 mm/rev; dry]

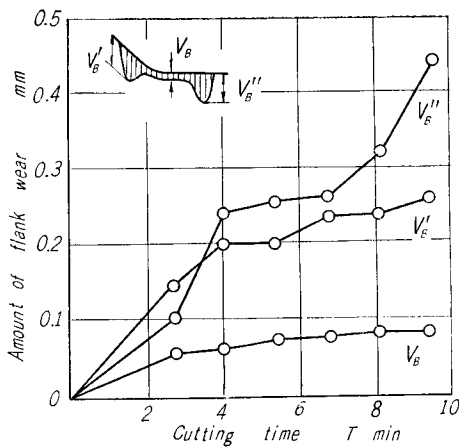


Fig. 10(b). Progress of flank wear with cutting time for ceramic O-1 [Work material, S45C; tool geometry,  $-5^\circ$ ,  $-5^\circ$ ,  $5^\circ$ ,  $5^\circ$ ,  $15^\circ$ ,  $15^\circ$ , 0.8 mm; cutting speed, 1000 m/min; depth of cut, 0.50 mm; feed, 0.05 mm/rev; dry]

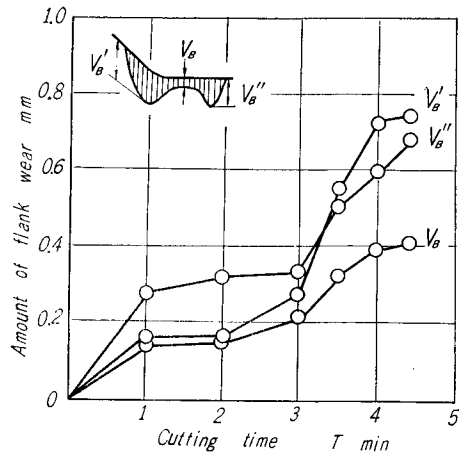


Fig. 11. Progress of flank wear with cutting time for cermet T-1 [Work material, S45C; tool geometry,  $-5^\circ$ ,  $-5^\circ$ ,  $5^\circ$ ,  $5^\circ$ ,  $15^\circ$ ,  $15^\circ$ , 0.8 mm; cutting speed, 1000 m/min; depth of cut, 0.50 mm; feed, 0.05 mm/rev; dry]

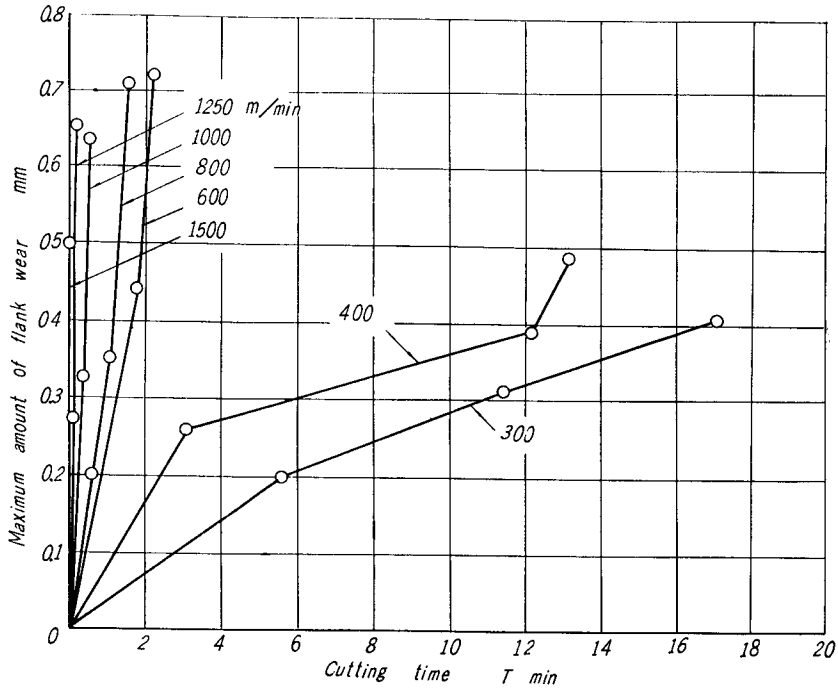


Fig. 12. Relationship between cutting time and the maximum amount of flank wear for carbide C-1 (steel cutting grade) [Work material, S45C; tool geometry,  $-5^\circ$ ,  $-5^\circ$ ,  $5^\circ$ ,  $5^\circ$ ,  $15^\circ$ ,  $15^\circ$ , 0.8 mm; depth of cut, 0.50 mm; feed, 0.05 mm/rev; dry]

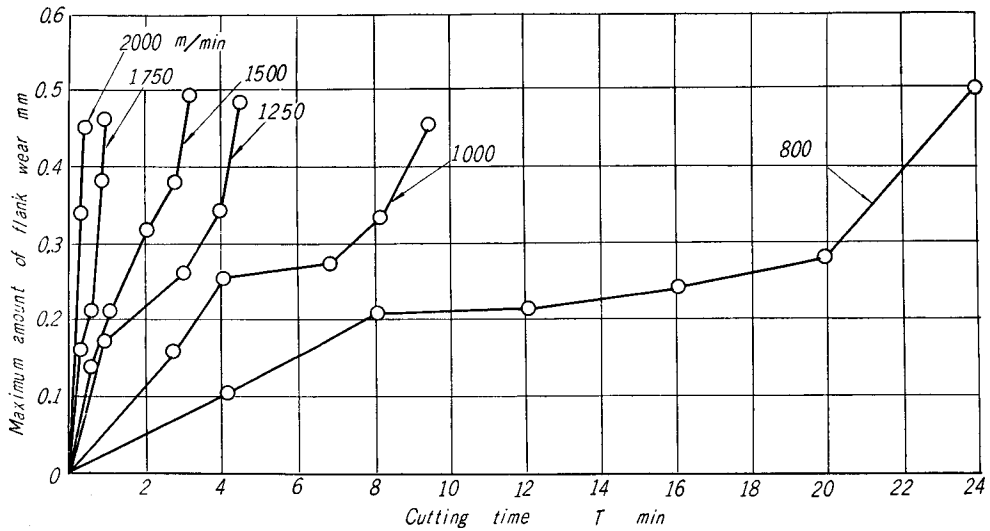


Fig. 13. Relationship between cutting time and the maximum amount of flank wear for ceramic O-1 [Work material, S45C; tool geometry,  $-5^\circ$ ,  $-5^\circ$ ,  $5^\circ$ ,  $5^\circ$ ,  $15^\circ$ ,  $15^\circ$ , 0.8 mm; depth of cut, 0.50 mm; feed, 0.05 mm/rev; dry]

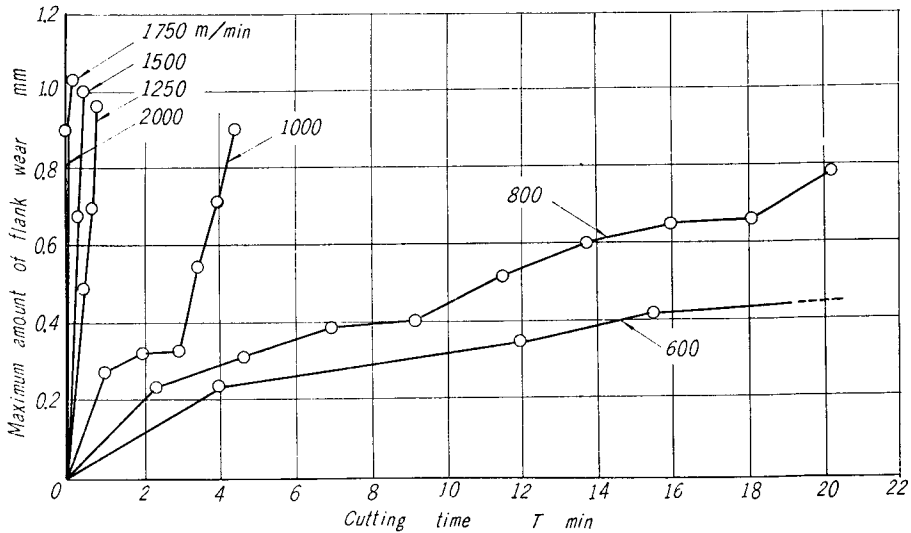


Fig. 14. Relationship between cutting time and the maximum amount of flank wear for cermet T-1 [Work material, S45C; tool geometry,  $-5^\circ$ ,  $-5^\circ$ ,  $5^\circ$ ,  $5^\circ$ ,  $15^\circ$ ,  $15^\circ$ , 0.8 mm; depth of cut, 0.50 mm; feed, 0.05 mm/rev; dry]

wear which is chipping appearing at low speeds and the cutting time in this primary wear stage decreased with an increase in cutting speed. At cutting speeds above 600 m/min for carbide C-1, 1250 m/min for cermet T-1, and 1750 m/min for ceramic O-1, the secondary type of flank wear which is caused mostly by the heat generated occurred in an instantaneous period of cut without accompanying the primary wear stage. It appears that the cutting temperature rises extremely at super-high speeds. This causes the sudden drop in hardness of tool materials. In addition, the vibration of the machine tool promotes the mechanical chipping at high speeds.

The relationship between cutting speed and tool life for a flank wear land of 0.40 mm is shown in Fig. 15 as Taylor tool-life curves on bilogarithmic paper. The empirical formulae indicating Taylor tool-life equation are shown in Table 3. It is found that the slope of tool-life curves is smaller at high speeds than at low speeds. Hence, the rate of decrease in tool life is great with an increase in cutting speed at super-high speeds. The ceramic tool O-1 showed the longest tool life among three kinds of tool materials, and had a tool life enough for practical use even at cutting speeds above 1000 m/min. It is expected to be used for super-high speed machining with proper tool geometry and cutting conditions. The cermet tool T-1 was not so good as the ceramic tool O-1 at high speeds, but at cutting speeds below 350 m/min it showed longer tool life than the ceramic tool O-1. The cermet tool is quite within the bounds of possibility for

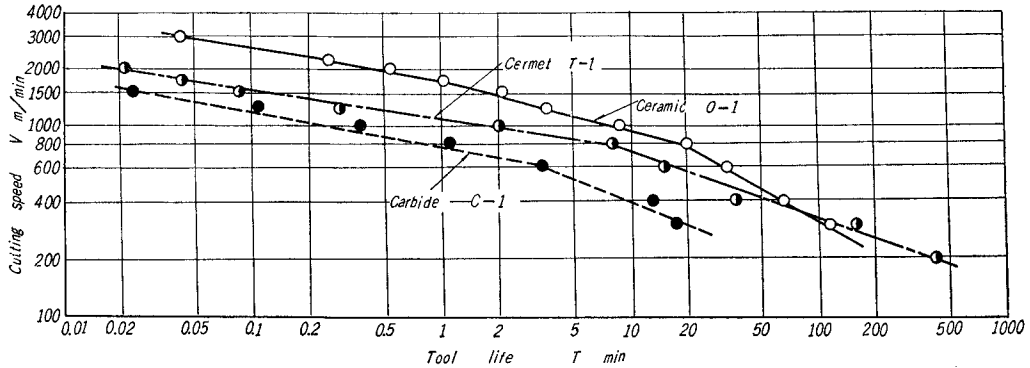


Fig. 15. Tool-life curves in super-high speed machining [Tool material, carbide C-1 (steel cutting grade), cermet T-1, and ceramic O-1; tool geometry,  $-5^\circ, -5^\circ, 5^\circ, 5^\circ, 15^\circ, 15^\circ, 0.8$  mm; work material, S45C; depth of cut, 0.50 mm; feed, 0.05 mm/rev; dry; tool-life criterion, flank wear of 0.40 mm]

Table 3. Empirical formulae indicating Taylor tool-life equation [Tool life criterion, flank wear of 0.40 mm; tool material, carbide C-1 (steel cutting grade), cermet T-1, and ceramic O-1; tool geometry,  $-5^\circ, -5^\circ, 5^\circ, 5^\circ, 15^\circ, 15^\circ, 0.8$  mm; work material, S45C; depth of cut, 0.50 mm; feed, 0.05 mm/rev; dry].

Tool material	Cutting speed (m/min)	Tool-life equation
Carbide C-1 (steel cutting grade)	300~ 600	$VT^{0.378} = 906$
	600~1500	$VT^{0.199} = 746$
Cermet T-1	200~ 800	$VT^{0.325} = 1718$
	800~2000	$VT^{0.145} = 1074$
Ceramic O-1	300~ 800	$VT^{0.562} = 4157$
	800~1750	$VT^{0.267} = 1767$
	1750~3000	$VT^{0.163} = 1752$

super-high speed machining above 1000 m/min with the improvement in tool geometry and utilization of proper cooling methods. On the other hand, the carbide tool C-1 damaged with a very short cut at super-high speeds. The practical speed limit for it was about 600 m/min.

### 5. Surface Roughness Experiments

Producing better surface finish is one of the important objectives in super-high speed machining. Since an excellent surface finish is obtained in grinding operation because of high speed cutting, super-high speed turning operation is expected to produce surface finish as good as by grinding in spite of a cutting

with a single-point cutting tool. In the following, the possibility of super-high speed machining will be discussed from the standpoint of surface roughness, conducting cutting tests on carbon steel S45C with carbide C-1, cermet T-1, and ceramic O-1. Tests were run dry under the following cutting conditions :

Depth of cut : 0.10 to 0.90 mm  
 Feed : 0.012 to 0.100 mm/rev  
 Cutting speed : 150 to 1000 m/min for carbide C-1  
                   150 to 1250 m/min for cermet T-1  
                   150 to 2000 m/min for ceramic O-1

Each run was started with a new cutting edge in this experiment and the surface roughness (the maximum height) along the initial cutting length of about 20 mm was measured with a Talysurf surface roughness indicator. Hence, the effect of the tool wear on the surface roughness was negligible except at extremely high cutting speeds.

Fig. 16 shows the surface roughness in relation to depth of cut. Although the surface roughness values decreased slightly with an increase in depth of cut, this effect on surface roughness was not so remarkable. The relationship between cutting speed and surface roughness is shown in Figs. 17 to 19 with a parameter of feed rate. It is found that the surface finish was improved with a decrease in feed rate. But, at a very small feed rate, it deteriorated in many

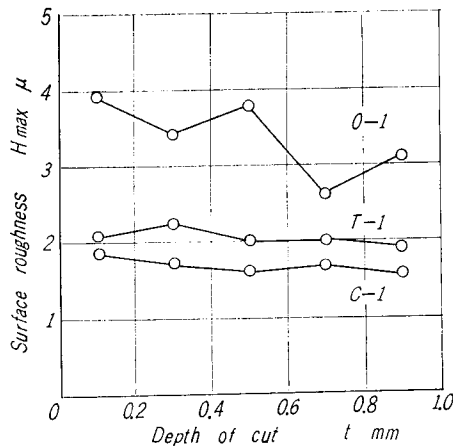


Fig. 16. Effect of depth of cut on surface roughness [Tool material, carbide C-1 (steel cutting grade), cermet T-1, and ceramic O-1; tool geometry,  $-5^\circ$ ,  $-5^\circ$ ,  $5^\circ$ ,  $5^\circ$ ,  $15^\circ$ ,  $15^\circ$ , 0.8 mm; work material, S45C; cutting speed, 1000 m/min; feed, 0.05 mm/rev; dry]

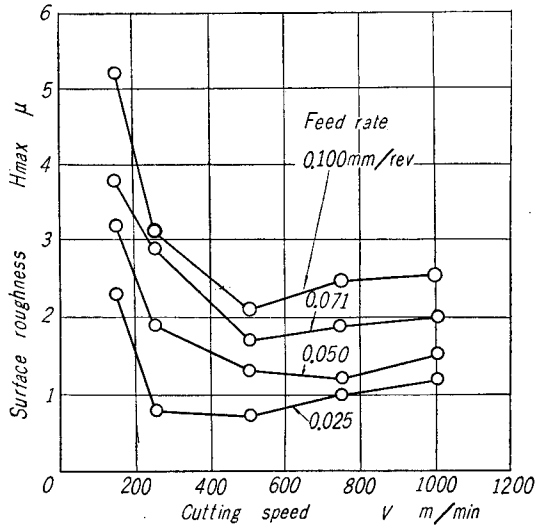


Fig. 17. Relationship between cutting speed and surface roughness for carbide C-1 (steel cutting grade) [Work material, S45C; tool geometry,  $-5^\circ$ ,  $-5^\circ$ ,  $5^\circ$ ,  $5^\circ$ ,  $15^\circ$ ,  $15^\circ$ ; 0.8 mm; depth of cut, 0.50 mm; dry]

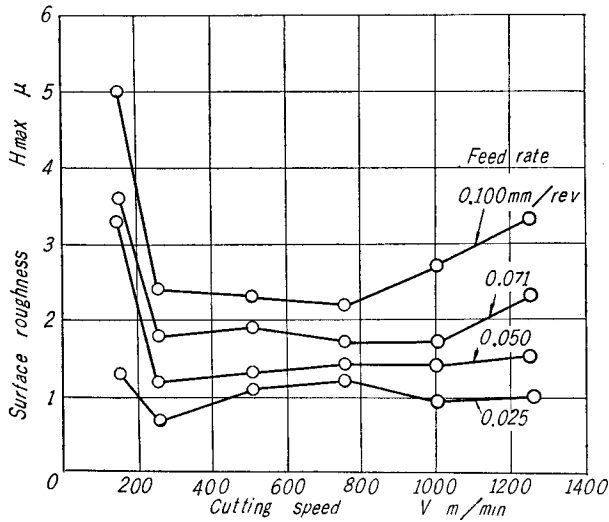


Fig. 18. Relationship between cutting speed and surface roughness for cermet T-1 [Work material, S45C; tool geometry,  $-5^\circ$ ,  $-5^\circ$ ,  $5^\circ$ ,  $5^\circ$ ,  $15^\circ$ ,  $15^\circ$ ; 0.8 mm; depth of cut, 0.50 mm; dry]



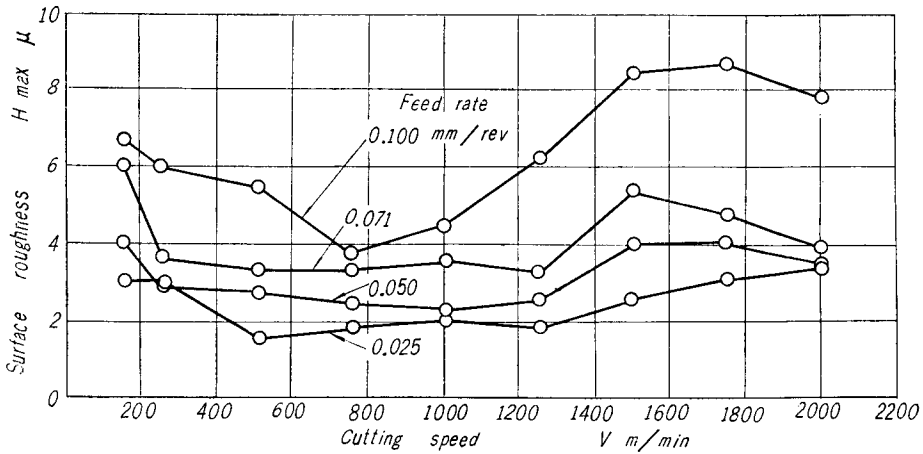


Fig. 19. Relationship between cutting speed and surface roughness for ceramic O-1 [Work material, S45C; tool geometry,  $-5^\circ$ ,  $-5^\circ$ ,  $5^\circ$ ,  $5^\circ$ ,  $15^\circ$ ,  $15^\circ$ , 0.8 mm; depth of cut, 0.50 mm; dry]

cases. This was caused by inaccuracy of the feed mechanism of the machine tool, the side flow effect, the size effect, etc. at small feed rates.

The roughness factor, the ratio of the actual surface roughness value to the theoretical surface roughness value\*, increased in exponential relationship with a decrease in feed rate.

It is concluded from the above that the optimum feed rate for obtaining the best surface finish is around 0.025 mm/rev.

The pattern of surface roughness in relation to cutting speed was similar for every feed rate tested. Surface roughness values were almost constant and smaller at cutting speeds of 250 m/min to 1000 m/min for carbide C-1 and cermet T-1 and 250 m/min to 1250 m/min for ceramic O-1 than at cutting speeds below 250 m/min. But, the surface roughness became worse at cutting speeds higher than these cutting speed ranges. The vibration of the machine tool due to its lack in rigidity appears to be a main reason for this. Consequently, in the present tests the surface finish was best in a cutting speed range of 250 m/min to 1000 m/min.

As shown in Fig. 20, machined surface profiles having regular feed marks were obtained with carbide C-1 and ceramic O-1. But irregular profile for the machined surface was noticeable at high cutting speeds and small feed rates. A large waviness was remarkable on the surface profiles for the cermet T-1, in spite of the smallest height of surface roughness among three kinds of tool

\* This is determined geometrically by tool geometry and feed rate.

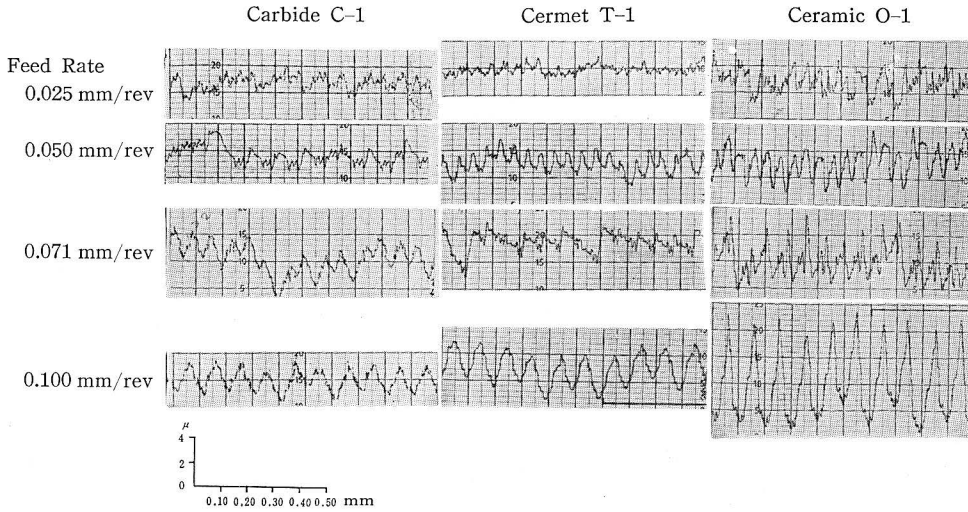


Fig. 20. Examples of profile of the machined surface in super-high speed machining [Tool material, carbide C-1 (steel cutting grade), cermet T-1, and ceramic O-1; tool geometry,  $-5^\circ$ ,  $-5^\circ$ ,  $5^\circ$ ,  $5^\circ$ ,  $15^\circ$ ,  $15^\circ$ , 0.8 mm; work material, S45C; cutting speed, 1000 m/min; depth of cut, 0.50 mm; dry]

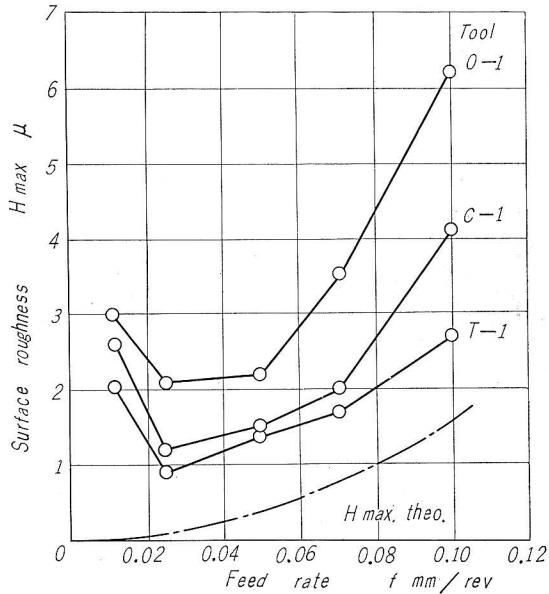


Fig. 21. Effect of feed rate on surface roughness [Tool material, carbide C-1 (steel cutting grade), cermet T-1, and ceramic O-1; tool geometry,  $-5^\circ$ ,  $-5^\circ$ ,  $5^\circ$ ,  $5^\circ$ ,  $15^\circ$ ,  $15^\circ$ , 0.8mm; work material, S45C; cutting speed, 1000 m/min; depth of cut, 0.50 mm; dry]

materials (Fig. 21). The surface roughness value for the ceramic O-1 was the largest.

### 6. Effect of Cutting Fluids

It is well known that cutting fluids are effective for the improvement of tool life and surface finish in low cutting speeds due to lubrication and cooling effects. In super-high speed machining application of an effective cooling method is expected to increase the tool life, since the tool life in this case is extremely shortened by the heat generated at super-high speeds. A supply of cutting fluids having a strong cooling ability into the cutting area is an easiest method to decrease cutting temperature in practical machining. Experimental results on super-high speed machining of carbon steel S45C by cermet T-1 and ceramic O-1 with supply of two kinds of cutting fluids, chemical solution type (dilution  $\times 10$ ) and soluble oil type (dilution  $\times 30$ ), are compared with test results in dry cutting, from the viewpoint of tool life and surface roughness. The cutting fluids were supplied continuously into the cutting area from the flank of a cutting tool in mist spray through a nozzle by compressed air of 2 atmospheric pressures at the rate of about 80 ml/min. For tool-life tests, depth of cut and feed rate were kept constant: 0.50 mm and 0.05 mm/rev, respectively, and cutting speed was varied: 400 m/min to 3000 m/min. For surface roughness tests, depth of cut was kept constant: 0.50 mm. Feed rate was varied: 0.012 mm/rev to 0.100 mm/rev. Cutting speed was also varied: 150 m/min to 1300 m/min for cermet T-1 and 150 m/min to 1500 m/min for ceramic O-1.

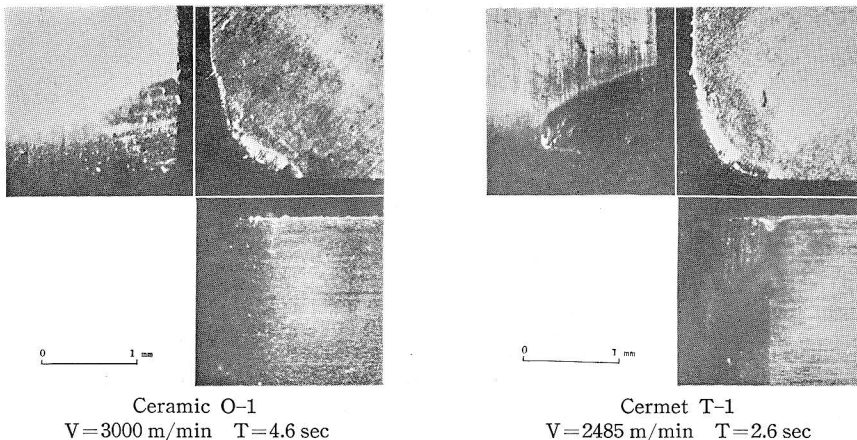


Fig. 22. Examples of tool wear process in super-high speed machining for wet condition [Tool material, ceramic O-1 and cermet T-1; tool geometry,  $-5^\circ$ ,  $-5^\circ$ ,  $5^\circ$ ,  $5^\circ$ ,  $15^\circ$ ,  $15^\circ$ , 0.8 mm; work material, S45C; depth of cut, 0.50 mm; feed, 0.05 mm/rev; cutting fluid, chemical solution type]

Comparing the test results for dry and wet cuttings at super-high speeds, no difference in the wear process on the tool face was observed (Fig. 22). In super-high speed machining, velocity of chip flow is extremely great and the contact area of chip on the tool face is very small and located near the cutting edge. It seems that these facts prevent the cutting fluids from penetrating into the cutting area under high pressure.

Figs. 23 and 24 show examples of the flank wear progress with cutting time for wet cutting. Both cermet and ceramic tools showed a similar pattern of the flank wear process for dry and wet cuttings at cutting speeds above 2000 m/min for the cermet T-1 and 2500 m/min for the ceramic O-1. It is found, however, that the rate of increase in the boundary flank wear for the ceramic O-1 was larger in wet cutting than in dry cutting at cutting speeds below 2500 m/min. The tool life in wet condition was about 1/3 to 1/4 of that in dry condition. The flank wear land at the nose of the cermet T-1 increased at high rate even at low speeds when cutting fluids were supplied. It is obvious from these facts that the boundary flank wear on the side of the ceramic tool O-1 and the chipping wear on the nose of the cermet tool T-1 are promoted by hardened grains in the chip and in the work material which were produced by cooling effect of cutting fluids.

A distinct difference in the wear process for cermet T-1 and ceramic O-1 was not noticed between the cutting fluids of chemical solution type and soluble oil type.

Results of tool-life tests for both dry and wet cuttings are shown in Fig. 25 as Taylor tool-life curves on bilogarithmic paper, showing the relationship between cutting speed and tool life based upon a flank wear land of 0.40 mm. The empirical formulae indicating Taylor tool-life equation are indicated in Table 4.

The slope of tool-life curves is slightly steeper for wet cutting than for dry cutting. But the tool life itself is shorter in wet cutting than in dry cutting at cutting speeds below 2000 m/min. At cutting speeds above 2000 m/min, however, the difference in tool life values for dry and wet cuttings was not distinct, and the cutting in wet condition often showed longer tool life than in dry cutting. Further detailed experiments are needed to conclude effects of cutting fluids on the tool life at high speeds, since in the above the tool-life tests for wet cutting were not conducted so many times as in the case of dry cutting.

It was observed that the soluble oil type cutting fluid containing a large percentage of water showed better tool life than the chemical solution type cutting fluid for both cermet T-1 and ceramic O-1.

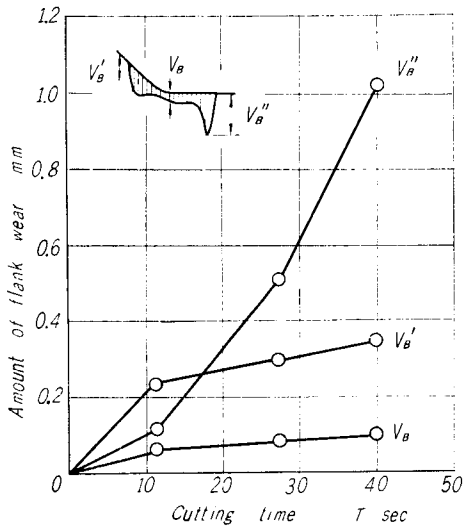


Fig. 23(a). Progress of flank wear with cutting time for ceramic O-1 in wet cutting [Tool geometry,  $-5^\circ$ ,  $-5^\circ$ ,  $5^\circ$ ,  $5^\circ$ ,  $15^\circ$ ,  $15^\circ$ , 0.8 mm; work material, S45C; cutting speed, 2125 m/min; depth of cut, 0.50 mm; feed, 0.05 mm/rev; cutting fluid, chemical solution type]

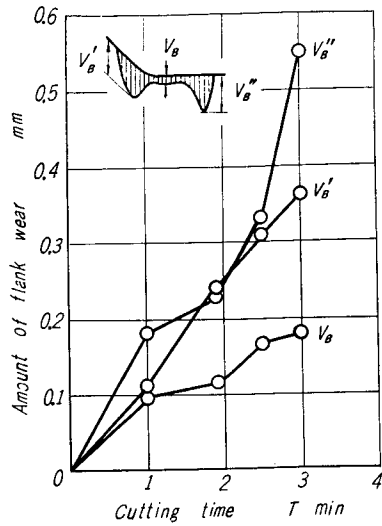


Fig. 23(b). Progress of flank wear with cutting time for ceramic O-1 in wet cutting [Tool geometry,  $-5^\circ$ ,  $-5^\circ$ ,  $5^\circ$ ,  $5^\circ$ ,  $15^\circ$ ,  $15^\circ$ , 0.8 mm; work material, S45C; cutting speed, 980 m/min; depth of cut, 0.50 mm; feed, 0.05 mm/rev; cutting fluid, chemical solution type]

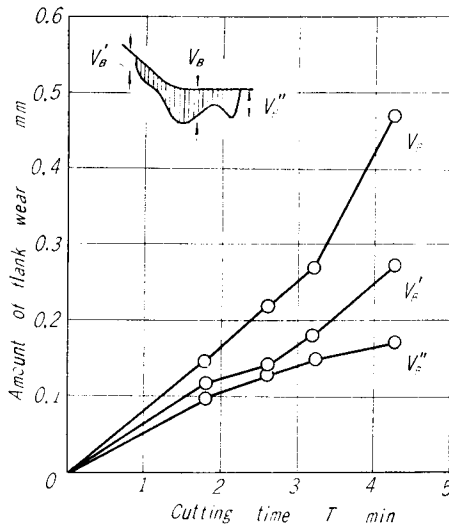


Fig. 24. Progress of flank wear with cutting time for cermet T-1 in wet cutting [Tool geometry,  $-5^\circ$ ,  $-5^\circ$ ,  $5^\circ$ ,  $5^\circ$ ,  $15^\circ$ ,  $15^\circ$ , 0.8 mm; work material, S45C; cutting speed, 790 m/min; depth of cut, 0.50 mm; feed, 0.05 mm/rev; cutting fluid, soluble oil type]

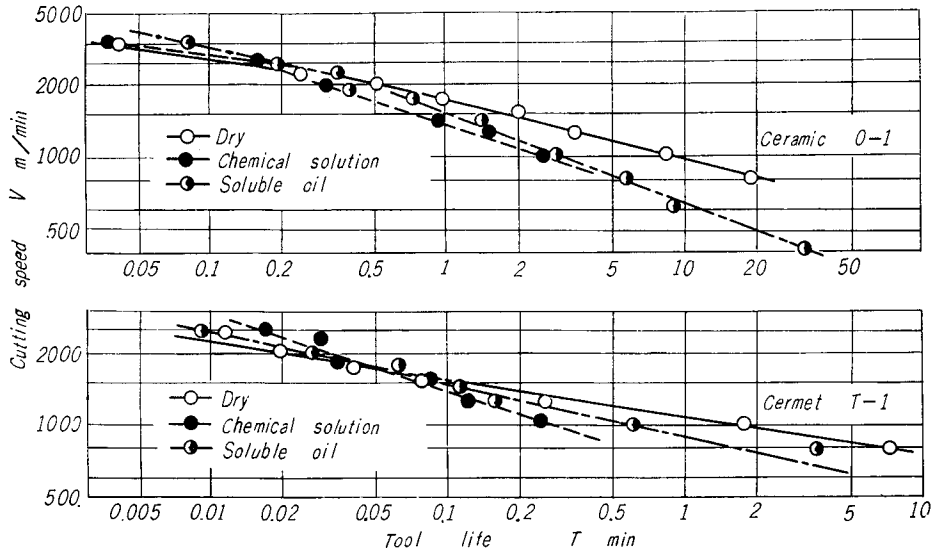


Fig. 25. Comparison of tool-life curves for dry and wet conditions in super-high speed machining [Tool material, cermet T-1 and ceramic O-1; tool geometry,  $-5^\circ$ ,  $-5^\circ$ ,  $5^\circ$ ,  $5^\circ$ ,  $15^\circ$ ,  $15^\circ$ , 0.8 mm; work material, S45C; depth of cut, 0.50 mm; feed, 0.05 mm/rev; cutting fluid, chemical solution type and soluble oil type; tool-life criterion, flank wear of 0.40 mm]

Table 4. Empirical formulae indicating Taylor tool-life equation for dry and wet cuttings [Tool material, cermet T-1 and ceramic O-1; tool geometry,  $-5^\circ$ ,  $-5^\circ$ ,  $5^\circ$ ,  $5^\circ$ ,  $15^\circ$ ,  $15^\circ$ , 0.8 mm; work material, S45C; depth of cut, 0.50 mm; feed, 0.05 mm/rev; cutting fluid, chemical solution type and soluble oil type; tool-life criterion, flank wear of 0.40 mm].

Tool material	Cutting fluid	Cutting speed (m/min)	Tool-life equation
Cermet T-1	Dry	800~2500	$VT^{0.145} = 1074$
	Chemical solution type	1000~2500	$VT^{0.322} = 659$
	Soluble oil type	800~2500	$VT^{0.224} = 890$
Ceramic O-1	Dry	800~2000	$VT^{0.267} = 1767$
		2000~3000	$VT^{0.163} = 1752$
	Chemical solution type	1000~2500	$VT^{0.330} = 1372$
		2500~3000	$VT^{0.122} = 2005$
	Soluble oil type	400~1750	$VT^{0.386} = 1536$
		1750~3000	$VT^{0.206} = 1782$

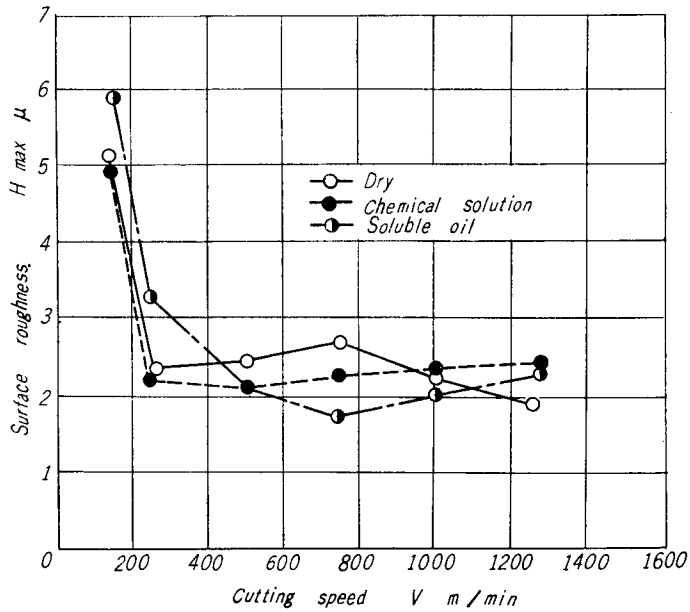


Fig. 26. Comparison of surface roughness in relation to cutting speed for dry and wet conditions in the case of cermet T-1 [Tool geometry,  $-5^\circ$ ,  $-5^\circ$ ,  $5^\circ$ ,  $5^\circ$ ,  $15^\circ$ ,  $15^\circ$ , 0.8 mm; work material, S45C; depth of cut, 0.50 mm; feed, 0.05 mm/rev; cutting fluid, chemical solution type and soluble oil type]

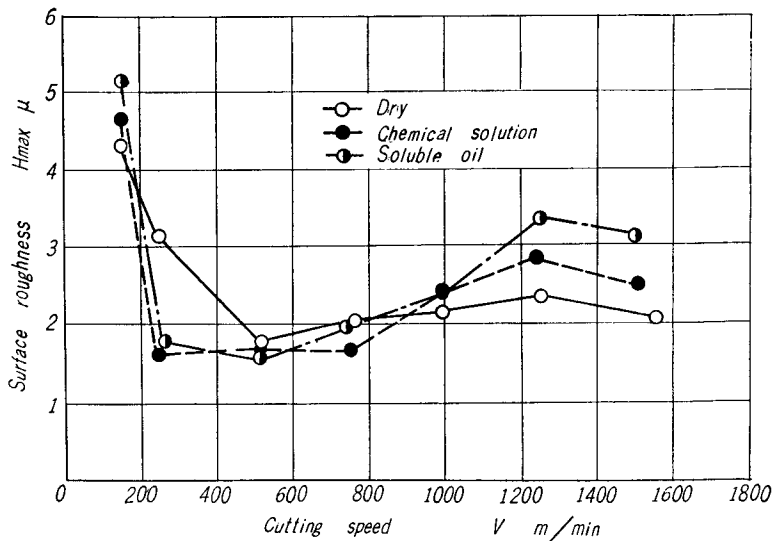


Fig. 27. Comparison of surface roughness in relation to cutting speed for dry and wet conditions in the case of ceramic O-1 [Tool geometry,  $-5^\circ$ ,  $-5^\circ$ ,  $5^\circ$ ,  $5^\circ$ ,  $15^\circ$ ,  $15^\circ$ , 0.8 mm; work material, S45C; depth of cut, 0.50 mm; feed, 0.05 mm/rev; cutting fluid, chemical solution type and soluble oil type]

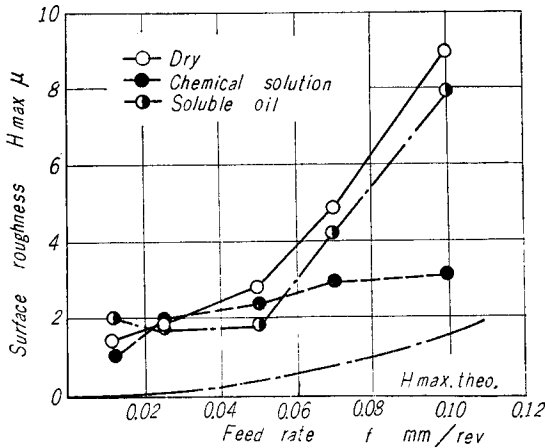


Fig. 28. Comparison of effect of feed rate on surface roughness for dry and wet conditions in the case of cermet T-1 [Tool geometry,  $-5^\circ$ ,  $-5^\circ$ ,  $5^\circ$ ,  $5^\circ$ ,  $15^\circ$ ,  $15^\circ$ , 0.8 mm; work material, S45C; depth of cut, 0.50 mm; cutting speed, 750 m/min; cutting fluid, chemical solution type and soluble oil type]

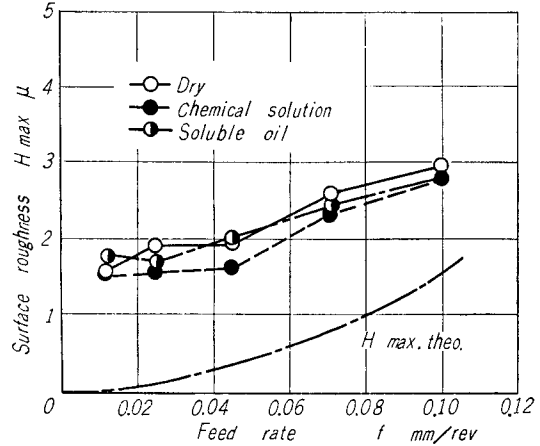


Fig. 29. Comparison of effect of feed rate on surface roughness for dry and wet conditions in the case of ceramic O-1 [Tool geometry,  $-5^\circ$ ,  $-5^\circ$ ,  $5^\circ$ ,  $5^\circ$ ,  $15^\circ$ ,  $15^\circ$ , 0.8 mm; work material, S45C; depth of cut, 0.50 mm; cutting speed, 750 m/min; cutting fluid, chemical solution type and soluble oil type]

Effects of cutting fluids on surface roughness at super-high speeds were also investigated. The relationship between surface roughness and cutting speed for wet and dry cuttings is shown in Figs. 26 and 27. It is found that both cermet T-1 and ceramic O-1 showed similar trend in surface roughness vs. cutting speed relationship. The wet cutting produced slightly better surface finish than the dry cutting at cutting speeds of 250 m/min to 1000 m/min. A contrary result was obtained outside this cutting speed range.

Cutting fluids were slightly effective to the improvement of the surface finish for each feed rate tested (Figs. 28 and 29). But the difference between surface roughness values for dry and wet cuttings was very small, except at a feed rate of 0.10 mm/rev for the cermet T-1.

It is concluded from the above that the cutting fluids do not have remarkable effect on the surface roughness at super-high speeds. This is because the super-high speed machining itself improves the surface finish to a great extent due to the improvement in cutting mechanism, increasing the cutting ratio and reducing the contact area of the chip on the tool face.

## 7. Conclusions

Cutting tests at super-high speeds were conducted on carbon steel with carbide, cermet, and ceramic tools, in order to investigate fundamentals of super-high speed machining. This leads to the following conclusions.



(1) The tool forces at super-high speeds were smaller than those at conventional speeds and almost constant with an increase in cutting speed.

The cutting time up to the beginning of tool force increase can be used as a criterion to determine an adequate tool material for super-high speed machining. It was found that the ceramic tool O-1 was more suitable for super-high speed machining of carbon steel S45C than the other cutting tool materials tested.

(2) The tool life at super-high speeds is mainly affected by the cutting temperature and the vibration of machine tool produced by high cutting speed. The slope of tool-life curve at high speeds is smaller than that at low speeds.

The ceramic tool O-1, which has high heat resistance property, showed the best tool life among three kinds of tool materials tested at super-high speeds. It indicated no definite crater wear on the tool face and the chipping wear on the nose was extremely small even at high speeds.

The cermet tool T-1 was not so good as the ceramic tool O-1 for super-high speed machining from the standpoint of tool life. At high speeds a great chipping wear occurred on the front and the nose of this tool.

Since the carbide tool C-1 is lacking in heat resistance property, a large crater wear occurred rapidly on the tool face at super-high speeds. This increased tool forces rapidly and shortened tool life. The practical cutting speed for the carbide tool C-1 is limited up to several hundred meters per minute.

(3) A very smooth surface finish of several microns in the maximum height was produced at super-high speeds. The efficiency of finish operation can be increased by conducting the super-high speed machining.

It was found that the optimum cutting conditions for obtaining the best surface finish were about 250 m/min to 1000 m/min for cutting speed and around 0.025 mm/rev for feed rate. The effect of depth of cut on surface roughness was not remarkable. The surface roughness became worse at cutting speeds higher than this cutting speed range due to the vibration of the machine tool and the rapid tool wear.

(4) Almost no difference between dry and wet cuttings at super-high speeds was observed in the wear process on the tool face. This indicates that the cutting fluids do not easily penetrate into the cutting area because of a large velocity of chip flow at super-high speeds.

The flank wear, especially the boundary flank wear for the ceramic tool O-1 and the chipping wear at the nose of the cermet tool T-1 developed rapidly when cutting fluids were supplied. This was because grains in the chip and the work material were hardened owing to the cooling effects of cutting fluids.

Although the slope of the tool-life curve was slightly steeper for wet cutting than for dry cutting, the tool life itself was shorter in wet condition than in dry condition at cutting speeds below 2000 m/min.

The effect of cutting fluids on the surface roughness was not so remarkable at super-high speeds. Better surface finish was produced with cutting fluids at cutting speeds of 250 m/min to 1000 m/min.

#### **References**

- 1) H. G. Groat and A. Ashburn: *Ultra-High Speed Machining*; *American Machinist*, Vol. 104, February, 1960, pp. 111-126.
- 2) M. Kronenberg: *Zweiter Bericht über die Vervielfachung heute üblicher Schnittgeschwindigkeiten*; *Werkstattstechnik*, Vol. 51, 1961, pp. 133-141.
- 3) K. Yamada and N. Nakayama: *Ultra-High Speed Machining and its Technique*; *Science of Machine*, Vol. 13, 1961, pp. 779-782 and pp. 911-916.
- 4) R. L. Vaughn and R. T. Krueck: *Recent Development in Ultra-High Speed Machining*; *Collected Paper, 1960, Library Edition*, Vol. 60, Book 1, Paper No. 255, *American Society of Tool and Manufacturing Engineers*, 20 pp.
- 5) K. Okushima and K. Hitomi: *A Design of a Three-Component Tool Dynamometer*; *Memoirs of the Faculty of Engineering, Kyoto University*, Vol. 23, No. 4, 1961, pp. 321-334.